Integrative analysis of subcellular quantitative proteomics studies reveals functional cytoskeleton membrane-lipid raft interactions in cancer

Anup D. Shah[1], Kerry L. Inder[1], Alok K. Shah[1], Alexandre S. Cristino[1], Arthur B. McKie[2], Hani Gabra[2], Melissa J. Davis[3], Michelle M. Hill[1*]*

[1] The University of Queensland Diamantina Institute, The University of Queensland, Translational Research Institute, Brisbane, Queensland, 4102, Australia

[2] Ovarian Cancer Action Research Centre, Division of Cancer, Imperial College London Hammersmith Campus, London, United Kingdom

[3] Division of Bioinformatics, The Walter and Eliza Hall Institute of Medical Research, 1G Royal Parade, Parkville Victoria 3052, Australia

*** Corresponding authors:**

Melissa J Davis

Division of Bioinformatics, The Walter and Eliza Hall Institute of Medical Research, 1G Royal Parade, Parkville Victoria 3052, Australia

Tel: +61 (0) 3 9345 2597

Fax: +61 (0) 3 8344 7412

E-mail: davis.m@wehi.edu.au

Michelle M Hill

The University of Queensland Diamantina Institute, The University of Queensland

Level 5, Translational Research Institute, 37 Kent Street, Woolloongabba, 4102, Queensland, Australia

Tel: +61 (0)7 3443 7049

Fax: +61 (0)7 3443 5946

E-mail: m.hill2@uq.edu.au

Running title: Raft associated mechanisms of tumor development

Key words: Lipid raft, quantitative proteomics, cancer progression, computational biology, cytoskeleton

ABSTRACT

Lipid rafts are dynamic membrane micro-domains that orchestrate molecular interactions, and are implicated in cancer development. To understand the functions of lipid rafts in cancer we performed an integrated analysis of quantitative lipid raft proteomics datasets modeling progression in breast cancer, melanoma and renal cell carcinoma. This analysis revealed that cancer development is associated with increased membrane raft-cytoskeleton interactions, with around 40% of elevated lipid raft proteins being cytoskeletal components. Previous studies suggest a potential functional role for the raft-cytoskeleton in the action of the putative tumor suppressors PTRF/Cavin-1 and Merlin. To extend the observation, we examined lipid raft proteome modulation by an unrelated tumor suppressor Opioid Binding Protein Cell-adhesion Molecule (OPCML) in ovarian cancer SKOV3 cells. In agreement with the other model systems, quantitative proteomics revealed that 39% of OPCML-depleted lipid raft proteins are cytoskeletal components, with microfilaments and intermediate filaments specifically down-regulated. Furthermore, protein-protein interaction network and simulation analysis showed significantly higher interactions among cancer raft proteins compared to general human raft proteins. Collectively, these results suggest increased cytoskeleton-mediated stabilization of lipid raft domains with greater molecular interactions as a common, functional and reversible feature of cancer cells.

INTRODUCTION

All cancers share a list of common 'hallmarks',[1] suggesting a convergence of cellular mechanisms of malignant transformation. Similarly, metastatic progression involves universal phenotypic changes including epithelial mesenchymal plasticity, anchorage-independent survival, and the ability to establish pre-metastatic niche.[2] Common properties develop regardless of the causal oncogene or tumor suppressor gene or the tissue of origin, implying alteration of fundamental cellular mechanisms. A potential unifying mechanism may involve modulation of cholesterol and sphingolipid-rich membrane microdomains, commonly referred to as lipid rafts.[3] Raft localization is known to regulate molecular interactions, and hence the function, of signaling proteins involved in carcinogenesis, such as RAS, EGFR and HER2.[4-6] Membrane rafts have been implicated in the development and progression of several cancers including prostate,[7] breast,[8] lung[9] and colon cancer.[10] However, it is unclear whether lipid rafts share cross-cancer similarities in their protein expression profiles, and how lipid raft alterations promote cancer. To this end, we performed an integrative analysis of publicly available quantitative proteomics datasets which evaluated cancer-associated lipid raft proteome from breast cancer,[11] melanoma[12] and renal cell carcinoma (RCC).[13] Conversely, we also examined lipid raft proteome during the reversal of tumorigenic potential of cell, based on recent studies reporting lipid raft proteome alterations associated with tumor suppressors Polymerase I and Transcript Release Factor (PTRF)[14,15] and Merlin.[16] Here, we further investigated the universality of this phenomenon by applying a quantitative subcellular raft proteomics approach to the ovarian cancer tumor suppressor OPCML.

OPCML is a GPI-anchored protein localized to membrane rafts under normal physiological condition.[17] A comprehensive loss of heterozygosity analysis of 118 epithelial ovarian cancer (EOC) cases has identified inactivation of OPCML at 11q25 either due to CpG island methylation or due to allelic loss.[18] A recent independent TCGA study also confirms this

finding, where 92% of 489 high-grade serous ovarian cancers reported loss of OPCML expression.[19, 20] OPCML promoter methylation is proposed to be a diagnostic as well as prognostic marker in EOC.[21] OPCML inactivation appears to be crucial for EOC because recombinant OPCML therapy demonstrated inhibitory effect on tumor growth *in vivo*.[22] As a GPI anchored-protein, OPCML is entirely on the exo-facial leaflet of the plasma membrane, hence it is unable to directly mediate signal transduction. We recently found that OPCML negatively regulates a subset of receptor tyrosine kinases (RTKs) by altering their recycling and ubiquitin-mediated degradation via sequestration to lipid rafts.[20] However, the molecular mechanism linking OPCML tumor suppressor expression to altered RTK trafficking remains unclear. Here, we performed a quantitative lipid raft proteomics study to dissect raft-mediated mechanism of OPCML regulated tumor suppression. We also examined raft-associated mechanism of OPCML P95R, a common mutation resulting in substitution of Proline to Arginine at position 95, mediated regulation of adhesion potential of tumors.[18] Furthermore, to evaluate the connectedness of proteins in cancer rafts compared to general raft and total human proteome, we compared the topological properties of simulated protein-protein interaction networks.

MATERIALS AND METHODS

Comparison of lipid raft changes during cancer progression in various cancer types

To evaluate common changes in the lipid raft proteome during cancer progression, two publications reporting changes in lipid raft protein composition in breast cancer[11] and melanoma[12] development were identified from RaftProt.[23] RaftProt is a mammalian lipid raft proteome database which is a comprehensive collection of 117 raft proteomes derived from 69 cell and tissue types of 6 mammals.[23] Specifically, experiments utilizing quantitative proteomics strategy to understand raft changes during cancer progression were selected. A more recent renal cell carcinoma raft proteomics study,[13] which was not present in the current

version of RaftProt was also included in the analysis. Data from these three studies were pre-processed for an integrative analysis, including mapping to UniProt accessions as required, removing single peptide identifications, generating the same fold-change characterization (aggressive/less aggressive) and applying the same cut-off criteria for significant quantitative changes. Fold change criteria was set to > ± 1.5 for each of the three datasets. Protein abundance ratios for melanoma and breast cancer datasets were reversed to maintain consistency in the directionality of protein expression change with RCC raft proteomics datasets. We then carried out an overlap analysis on two distinct sets: up-regulated and down-regulated proteins from membrane rafts during malignant progression to define a set of 'core cancer lipid raft proteome'.

Cytoskeletal proteins enrichment analysis

Human proteins with gene ontology annotations for biological process, molecular function or cellular compartment having the keyword "Cytoskeleton" in Amigo 2.2.0[24] (accessed on May 12, 2015) were fetched. This yielded a set comprised of 8432 annotations mapping to 4393 unique cytoskeleton associated proteins out of 48293 human UniProtKB entries annotated by GO terms (**Supplemental Table S1**). This set was designated "cytoskeleton associated proteins" of the human proteome. A subset was created from above dataset by filtering lipid raft localized cytoskeletal proteins (684 proteins) mentioned in the "RaftProt".[23] The Pearson's X^2-square goodness of fit test was performed to characterize enrichment of cytoskeletal elements in our ovarian lipid raft proteomics data and in ovarian lipid raft localized protein-protein interaction network (methods described below) against above mentioned background sets.

Cell culture and Stable Isotope Labeling by Amino Acids in Cell Culture (SILAC)

SKOV3 cells were stably transfected with empty control vector, WT OPCML or P95R OPCML as described previously.[18] Cells were grown under 5% CO_2 at 37°C in RPMI/L-Glut

with 10% fetal calf serum and 125µg/mL Zeocin. For Stable Isotope Labeling by Amino Acids in Cell Culture (SILAC) experiments, cells were grown in media lacking lysine and arginine with 10% dialyzed fetal calf serum and supplemented with the following amino acids: Control SKOV3 cells, normal isotopic Lys and Arg ("0/0") designated as "Light"; P95R mutant expressing SKOV3 cells, $^{2}H_4$-Lys and $^{13}C_6{}^{14}N_4$-Arg ("4/6"), designated as "Medium" and WT OPCML expressing SKOV3 cells, $^{13}C_6{}^{15}N_2$-Lys and $^{13}C_6{}^{15}N_4$-Arg ("8/10") designated as "Heavy". Cells were grown for more than 200 doublings in the SILAC media to achieve >99% label incorporation as confirmed by liquid chromatography-tandem mass spectrometry (LC-MS/MS).

Isolation of lipid raft fraction

Lipid rafts were prepared using the detergent resistant membrane (DRM) extraction method as previously described.[14, 25-30] Equal amount of DRM proteins prepared from each cell line was combined to make a Triplex SILAC mixed sample. Three biological replicates were independently prepared using different passage cells. DRM proteins (30 µg of mixed sample) were separated by SDS-PAGE to eight fractions and in-gel tryptic digest was performed using a liquid handler as previously described.[26]

LC-MS/MS, Database Searching, SILAC Quantitation and Statistical Analysis

Digested samples were analyzed using a 1200 Series nano HPLC and Chip-Cube Q-TOF 6510 (Agilent Technologies). Peptides were separated on a 160 nl (75 mm * 150 µm) high capacity C18 reverse phase chip by a 55 min gradient from 0 to 45% acetonitrile with the Vcap 1850 V, fragmentor 175 V. Precursor ions were selected in the range of 100–3200 m/z and fragment ions at 59–3200 m/z; reference ion mix was applied. Triplex SILAC samples were analyzed in auto MS/MS mode, with 8 MS and 4 MS/MS per second. Mass spectra extraction, database searching, and relative abundance were performed using Spectrum Mill software (Agilent, B.04.00) against Human SwissProt database (release-2014_11 containing 20194

entries). Cysteine carbamidomethylation and SILAC amino acids N-Lys, $^{2}H_4$-Lys, $^{13}C_6{}^{15}N_2$-Lys, N-Arg, $^{13}C_6{}^{14}N_4$-Arg and $^{13}C_6{}^{15}N_4$-Arg were used as fixed/mix modifications and oxidized methionine was selected as variable modification. Other parameters were: up to 2 missed cleavages for trypsin; minimum of 4 detected peaks; ±20 ppm and ±50 ppm threshold for MS and MS/MS measurements respectively. Positive identification required a peptide score >10 and >60% scored peak intensity. The global peptide level FDR was kept at 0.5% for generating peptide summary from Spectrum Mill. Two SILAC ratios namely, L/H and L/M, were considered for peptide quantitation, representing protein expression changes upon ectopic expression of WT OPCML (H) and P95R OPCML (M), respectively, in the empty vector transfected SKOV3 cells (L).

Peptides representing known protein contaminants according to common Repository of Adventitious Proteins (cRAP version 2012.01.01)[31] were manually removed. At the same time, only proteins identified by two or more unique peptides were filtered and considered for the downstream statistical analysis. We then used this peptide level data against Quantitative Proteomics *p-value* Calculator (QPPC)[32] server to catalogue the significantly altered proteins in each pair-wise comparison. QPPC utilizes peptide level measurements to compute protein abundance and statistical significance using the permutation test. We recently demonstrated superiority of permutation test over other widely used statistical methods because it is not based on data normality assumption.[33] We selected 10,000 permutations, with an outlier removal threshold of 100 for the peptide based SILAC ratios along with two cut-off criterion namely, fold change threshold of ±1.5 and p-value < 0.05. Before proceeding to calculation of permutation based statistics, QPPC performs additional data preprocessing to eliminate (i) peptide ratios that are negative, not numbers or 0s; (ii) peptides that are the only single observation of its respective protein; and (iii) peptides that have measurements above the outlier threshold. Mean SILAC ratio and standard deviation for individual protein was

calculated for each of the two pair-wise comparisons namely, "Light/Heavy" (L/H) and "Light/Medium" (L/M) separately using QPPC. In order to account for experiment-to-experiment variability and to create a baseline for downstream relative abundance comparison between L/H and L/M pair-wise comparisons, a mean normalization was performed on protein ratios, based on average protein abundance within each pair-wise comparison, during the statistical analysis with QPPC (**Supplemental Figure S1**).

Generation of lipid raft associated protein-protein interaction network

A human protein-protein interaction network was downloaded from PINA 2.0 (version updated on May 21, 2014).[34] PINA is a resource of protein-protein interactions, created by compiling protein interaction data across six publicly available, manually curated databases: HPRD,[35] IntAct,[36] BioGRID,[37] MINT,[38] DIP[39] and MIPS MPact.[40] As the downloaded interactome does not contain all the OPCML binding proteins reported in the literature,[20] we added five interactions to the PINA network (OPCML interacting with each of HER2, HER4, FGFR1, FGFR3 and EPHA2).[20] We then took the list of all DRM proteins identified in our experiment (both those that change abundance, and those that do not), and built an "intra-raft" protein interaction network, consisting of only interactions within proteins identified in our experiment. Cytoscape 2.8.2 was used for network visualization and analysis.[41]

Next, protein measurements (abundance and statistical significance of altered expression) were overlaid on the ovarian raft associated protein-protein interaction network, together with the information about cytoskeleton association in Cytoscape. Three sub networks were then created: (a) Interactions among cytoskeleton associated proteins inside the lipid raft; (b) Interactions within significantly altered cytoskeleton associated proteins at the lipid raft upon WT OPCML expression; (c) Interaction network of first neighbor of significantly altered cytoskeletal proteins found in network (b) and analyzed using Cytoscape.

Statistical analysis of protein-protein interaction network topological properties

Permutation testing was used to determine the statistical significance the network properties of cancer raft networks compared with networks derived from the proteome of normal human rafts. One thousand protein-protein interaction (PPI) networks were generated by fetching experimentally validated interactions between 230 randomly sampled proteins (the total number of proteins identified in ovarian raft) from multiple datasets: the complete human proteome, human raft proteins (from RaftProt)[23] along with cancer raft datasets belonging to RCC[13] and prostate cancer lipid raft proteome.[14] Each of the thousand networks were built by retrieving interactions associated with each random protein set from the PINA2 human interactome. For each PPI network, we calculated the total number of nodes, total number of edges and average degree distribution using the igraph package in R (www.r-project.org).[42] The data generated from 1000 networks derived from the normal human raft proteome was used to generate a distribution of values. We then use a z-test to determine the significance of the properties of networks sampled from the human proteome and three cancer raft proteomes (ovarian cancer, prostate cancer and RCC).

RESULTS

Comparative analysis of lipid raft alterations during cancer progression

The potential role of lipid rafts, a platform that coordinates cellular events, in cancer development has been well characterized.[3, 43] However, with the advancements in quantitative proteomics techniques, spatio-temporal changes in the protein composition of these microdomains have just begun to unfold. Very little is known about the commonalities in the lipid raft protein components in different cancer types; understanding these shared features is critical to uncover pan-cancer mechanisms. To this end, we carried out an integrative analysis of quantitative lipid raft proteomics datasets that compared protein levels during tumorigenesis of breast cancer, melanoma and renal cell carcinoma (**Figure 1**).

Three quantitative lipid raft proteomics studies were selected for this analysis as outlined under methods section. These studies utilized different models and quantitation methods, although all studies used the detergent-resistant membrane method for lipid raft extraction. Baruthio *et al.*,[12] examined raft associated changes in protein expression during melanoma progression using label-free proteomics technique. In this dataset, spectral counts from four cell lines of different metastatic potential i.e. MEK representing pre-malignant cells, SBCL representing primary tumor and SMel93 and WMFG cells representing malignant melanoma cells at different time points (for SBCL cell line) were pooled together to calculate the relative abundance of lipid raft related proteins. A criterion of at-least one observation in comparison between either pre-malignant (SBCL or MEK) or malignant cell type (SMel93 and WMFG) was used to characterize proteins altered during melanoma progression. Caruso *et al.,*[11] carried out proteomic profiling of lipid raft in breast cancer model of tumorigenic progression (MCF10A cell lineage) using iTRAQ based quantitative proteomics. Although relative quantitation of lipid raft proteins for pre-malignant cell lines (MCF10AT and MCF10ATG3B) were available, we only considered proteins altered in fully malignant MCF10CA1a cell line compared to parent MCF10A cells for the purpose of this study. Raimondo and co-workers[13] have characterized differential raft associated proteins in renal cell carcinoma (RCC) tissue samples compared to adjacent normal kidney (ANK) tissues with the help of label free proteomics.

Data from these three studies were pre-processed for integrative analysis, generating the same fold-change ratio (more aggressive/less aggressive). Taking the fold change cut-off of ±1.5, a total of 310 unique differentially regulated raft proteins were identified across the three published cancer progression model studies in breast cancer, melanoma and RCC (**Supplemental Table S2**). There were 159 unique under-expressed and 170 over-expressed proteins in aggressive cancer cell or tissues, with some proteins showing opposite regulation

in different datasets (**Figure 2).** To distil the data into a 'core cancer lipid raft proteome', proteins consistently altered in at-least two out of three datasets were selected (**Table 1)**. Out of the 23 altered raft proteins, 19 proteins were elevated in malignant lipid rafts, while 4 proteins were reduced during tumor progression (**Figure 2a and 2b**). This finding suggests that there are similarities in association/enrichment of specific repertoire of raft proteins in highly malignant tumours. Moreover, 12 of these 23 proteins are structural, regulatory or effector components of cytoskeleton (RAC1, AHNAK, GNAI2, GNAI3, GBG12, GAPDH, GELS, STOM, FLOT2, ENPL and PLEC).

To compare the extent of up-regulation of cytoskeletal proteins inside DRM across the three proteomics datasets during cancer progression, we further calculated the proportion of cytoskeleton associated proteins up-regulated in the lipid raft in each cancer types based on the GO annotation. Cytoskeleton proteins represent 36%, 45% and 31% of differentially modulated raft proteins in breast cancer, RCC and melanoma respectively during malignant progression. These results suggest that altered cytoskeleton assembly at lipid rafts is a common phenomenon during cancer progression.

Ectopic expression of WT and P95R OPCML alters lipid raft proteome of SKOV3 cells

The above integrated analysis suggests that increased cytoskeleton assembly at lipid raft membranes is a common feature in cancer development and progression regardless of tissue of origin. If the cytoskeletal components clustered at lipid raft during malignant progression, then ectopic expression of raft associated tumor suppressor should reverse this association. We previously reported that expression of PTRF in prostate cancer PC3 cells reduced the level of the actin cytoskeleton and associated proteins in the lipid raft fraction, concomitant with reduced invasive properties.[14] Furthermore, recent studies using live cell imaging,[44] molecular dynamic simulations[45] and *in-vitro* studies[46] strongly advocate the role for cytoskeletal dynamics at the lipid raft as a mediator of cellular function.[47] To further evaluate the hypothesis

that limiting cytoskeleton assembly at lipid rafts is a common mechanism of lipid raft-associated tumor suppressors, we characterized the effect of the GPI-anchored tumor suppressor OPCML in ovarian cancer.

The lipid raft proteome of ovarian cancer SKOV3 cells expressing WT OPCML or a partially inactive cancer-associated mutant OPCML (P95R) was compared to control SKOV3 cells in a triplex SILAC subcellular proteomics experiment **(Figure 3a)**. The P95R mutation occurs at the first immunoglobulin domain of OPCML **(Figure 3b and 3c)** and results in loss of cell adhesion function of OPCML while retaining growth suppression function.[20] Equal amount of detergent-resistant membrane (DRM) fractions from different SILAC-labelled SKOV3 cells stably transfected with empty vector (no OPCML expression), WT OPCML or P95R mutant were combined and then analyzed by LC-MS/MS. The protein ratios were calculated from peptide SILAC ratios from the three independent experiments **(Supplemental Table S3).** Two pair-wise comparison lists were obtained: control (OPCML-negative) SKOV3 cells versus WT OPCML SKOV3 cells (L/H); control SKOV3 cells versus P95R OPCML (L/M). Overall, we quantified the expression profiles of 218 and 223 DRM proteins in the respective comparisons out of the total of 230 non-redundant proteins. Using the criteria of >±1.5 fold change with *p-value* < 0.05, we found 38 and 22 significantly altered DRM proteins by either WT OPCML or P95R OPCML, corresponding to 16.5% and 9.5% of total quantified proteins (**Supplemental Table S4, Figure 3d and 3e)**. Interestingly, WT OPCML and P95R OPCML expression mainly depleted DRM proteins (observed as a positive log ratio in the volcano plots **Figure 3d and 3e**); suggesting that the tumor suppression function of OPCML may be mediated by a reduction in lipid raft proteome interactions. The comparative analysis of overlapping altered proteins indicated that 17 proteins were depleted from DRM by both variants of OPCML (**Figure 3f**). In addition, WT OPCML by itself modulated 21 raft proteins, whereas P95R OPCML modulated raft association of 5 of total 22 altered proteins on its own

(**Figure 3f**). This indicates that the P95R mutation affects raft confinement of a subset of protein regulated by WT OPCML, in addition to playing a role in altering recruitment of some unique proteins not affected by WT OPCML.

To our knowledge, this is the first study to characterize the lipid raft assembly, on a proteome-wide scale, in a system of ovarian origin using mass spectrometry method. To determine the similarity of the ovarian lipid raft proteome with known lipid raft associated proteins, we compared the ovarian raft proteins to the human lipid raft proteins in the RaftProt database[23] which currently hosts 67 human lipid raft proteome datasets derived from 50 different cell or tissue types. Out of 230 unique ovarian lipid raft proteins, 220 proteins were present in RaftProt, with 192 (~84%) classified as high confidence *bona fide* lipid raft proteins, meaning they were identified by more than 1 lipid raft isolation methods or were reported to be sensitive to methyl-β-cyclodextrin extraction. Interestingly, 10 proteins were not detected in any of the 67 other high throughput MS based lipid raft proteomics experiments in RaftProt. These proteins are AMGO2, AT2C2, DHRS2, ERBB2/HER2, FGF2, H11, H2B1A, HS904, LDH6A and VAMP1 (**Supplemental Table S4**). The presence of ERBB2/HER2 in lipid rafts has previously been reported using western blotting and microscopic techniques.[20] Although further studies using complementary techniques are needed to confirm the other unique ovarian cancer raft proteins, it is likely that these proteins were not identified by mass spectrometry in previous proteomics studies due to their low abundance in lipid rafts in other tissues or cell types.

Enrichment of cytoskeletal associated proteins in the lipid rafts of ovarian cancer cells.

Cytoskeleton associated proteins were highly enriched in the ovarian cancer rafts, as this class represents 34% of the entire dataset. Of the 23 pan-cancer lipid raft proteins, 19 were observed in our ovarian raft datasets, including nine cytoskeleton associated proteins (**Table 1**). Similar to the findings from three cancer progression quantitative proteomics datasets, 39%

and 35% of DRM proteins altered by WT and P95R OPCML expression in ovarian cancer cells were cytoskeletal associated. To determine the extent of interaction between the raft proteins, an ovarian raft protein-protein interaction network was built using experimentally validated PPIs (**Supplementary Figure S2**). Around 80% of the raft proteins interact with each other. Furthermore, 87% of the ovarian raft cytoskeletal proteins interact with other raft residents, and tend to have a larger number of interactions. This is indicative of higher connectedness of this class of proteins within the rigid environment provided by membrane rafts. Statistical analysis showed that both the ovarian raft-proteome and the raft associated interaction network were significantly enriched with cytoskeleton associated proteins compared to the human lipid raft proteome and the whole human proteome **(Table 2)**.

As the ovarian raft-associated protein interaction network is enriched with cytoskeletal proteins, we then asked whether the ectopic expression of OPCML modulates their association with membrane-rafts. If we consider only cytoskeleton associated proteins from this network, we find a single, dense cluster of 54 interacting proteins (**Figure 4**). We visualize the changes in abundance of these interacting proteins under different treatment conditions to identify coordinated changes in the cytoskeleton-associated network (**Figure 4**). A repertoire of cytoskeletal proteins show up-regulation (green), down-regulation (magenta) or loss of expression (gray) upon WT OPCML expression (**Figure 4a**). The same pattern of protein expression changes was not seen with P95R OPCML (**Figure 4b**). This result also suggests that the WT and P95R OPCML differentially regulate actin filaments, intermediate filaments and cytoskeleton regulatory proteins, but microtubules (tubulins) were not significantly altered by WT or P95R OPCML.

We then focused on the WT OPCML-specific lipid raft cytoskeleton associated proteins, reasoning that these proteins may mediate the mechanism of OPCML-induced cell adhesion, since P95R OPCML has lost this property. The sub-network of WT OPCML-altered

cytoskeletal DRM proteins comprise of a cluster of six proteins **(Figure 4c and 4d)**. While actin microfilament regulating proteins PLEC, JUP and SPTAN1 were significantly down-regulated by WT and P95R OPCML expression, VIM, DES and PRPH were significantly down-regulated by WT but not P95R OPCML. These results suggest that the loss of VIM, DES and PRPH from rafts containing WT OPCML may be associated with the inhibition of cell adhesion. VIM and DES are intermediate filaments that are well characterized markers of mesenchymal phenotype observed among aggressive tumor cells.[48, 49] Depletion of VIM and DES from the ovarian rafts upon WT OPCML expression might reverse the epithelial to mesenchymal transition of SKOV3 cells.

To evaluate crosstalk between differentially regulated cytoskeletal components with non-cytoskeletal proteins, this significantly down-regulated network module (**Figure 4c**) was expanded to include neighboring interactions, resulting in a network of 25 proteins with 50 interactions (**Figure 5**). This expanded network includes other cytoskeleton associated proteins ACTB, ATCTA2, MYL6, MYH9, CCT6A, GNAI2 and FYN, as well as integrins ITGA6 and B4 and the receptor tyrosine kinase ERBB2. The down-regulation of raft localized ERBB2 by OPCML observed in this work corroborates our previous findings.[20] Furthermore, both WT and P95R OPCML expression reduced ERBB2 in DRM **(Figure 5a and 5b)**; suggesting ERBB2 removal from lipid rafts may be a mechanism for growth suppression by both WT and P95R OPCML, potentially mediated by reducing raft-actin microfilament interaction. On the other hand, WT but not P95R OPCML increased the DRM level of desmoglein-2 (DSG2), a component of intracellular desmosomal cadherins.[50] These results suggest that a web of interacting cytoskeletal components in the ovarian cancer rafts might influence the sequestration of proteins to the raft. To determine if this property is unique to our ovarian cancer data, or is seen in other types of cancer, we next evaluated interaction potential of lipid raft proteomes in two further models of cancer development.

Cancer lipid rafts: a signaling platform stabilized by protein-protein interactions

Lipid rafts are known to restrict lateral diffusion of proteins and thereby create a favorable environment for proteins to interact.[51] Cytoskeletal rearrangements can further influence raft protein clustering by stabilizing the raft assemblies.[52] Even though the role of the lipid raft as a coordinator of protein-protein interaction has been documented,[51, 53] very little is known about the interaction potential of these microdomains in cancer. Out of the 230 ovarian lipid raft proteins identified in the dataset of ovarian cancer, 183 proteins (~80%) interact with each other in the ovarian raft associated interaction network we described above **(Supplemental Figure S2**). To determine if this degree of connectivity is characteristic of cancer rafts and different from what might be expected of a normal raft proteome, we performed a series of network simulations comparing interactions between known raft proteins[23] to interactions in the wider human proteome and in three cancer lipid raft proteomes (ovarian cancer (this study), prostate cancer and RCC, **Supplemental Table S5**). We exclude breast cancer and melanoma raft proteomes due to the smaller size of their measured proteomes. The sample size of each dataset for network generation was normalized to the number of proteins detected in the ovarian lipid raft. Compared to the network properties (number of interacting proteins, number of interactions between proteins and average number of neighbor in the network) of the normal human raft interactome, the proteins from complete human proteome participate in significantly fewer interactions. Interestingly, all three cancer rafts showed significantly larger number of interactions (p-value < 0.05 for every topological measure) compared to the interactions between normal raft resident proteins (**Table 3**). These findings suggest that the proteins in cancer rafts have higher tendency to engage in interactions with the other raft resident proteins.

DISCUSSION

Mounting evidence supports a key role of lipid rafts in cancer development and progression in multiple cancer systems, with diverse molecular mechanisms proposed.[54] Numerous studies have documented the interplay between lipid raft and membrane cytoskeleton,[47, 52, 55] with a potential role in coordinating membrane-associated cellular events relating to tumor progression, such as motility, cell adhesion, signal transduction and receptor endocytosis.[56] Here we used integrative analysis of quantitative lipid raft proteomics to identify increasing abundance of raft-associated cytoskeletal proteins as an underlying molecular mechanism in cancer progression. In the comparative analysis of multiple cancer raft proteomes, we observed that cytoskeletal proteins dynamically partition to lipid rafts during cancer development. These cytoskeletal components are considered to alter membrane heterogeneity by tethering the membrane raft components to intra-cellular structures,[57] thereby stabilizing raft microdomains.

If lipid raft-cytoskeleton interactions drive tumor progression, the corollary is that tumor suppressors acting on lipid rafts should reduce the cytoskeleton attachment. In a previous study, we reported such phenomena for PTRF/cavin-1 in prostate cancer PC3 cells,[14] while an independent report suggest that merlin, the neurofibromatosis-2 gene product also acts by disrupting cytoskeleton-lipid raft interaction.[16, 58] Here we report similar findings for an unrelated tumor suppressor, OPCML, in ovarian cancer. Together these results indicate that the lipid raft cytoskeleton association is critical for tumor progression. Further, ectopic expression or drug induced expression of raft localized tumor suppressor molecules might reverse neoplastic transformation through re-organizing cytoskeletal components inside membrane microdomains.

Due to their abundance, cytoskeleton components are commonly observed in lipid raft proteomics studies. By quantitatively comparing lipid raft proteome changes induced by ectopic expression of WT and P95R OPCML in SKOV3 cells, which led to differing adhesive properties,[18] we identified a potential involvement of intermediate filament-lipid raft

interaction for tumor adhesion. Expression of either WT or P95R OPCML in SKOV3 cells reduces cell proliferation but only WT OPCML imparts cellular adhesion. Intriguingly, both cell lines showed reduction of lipid raft actin microfilament regulating proteins (PLEC, JUP and SPTAN1), while intermediate filament proteins (VIM and DES) and tetraspanin-22 (PRPH) were down-regulated by WT but not P95R OPCML. VIM is a well characterized marker of epithelial-to-mesenchymal transition (EMT) during cancer progression.[59] In ovarian cancer tissues, VIM expression is significantly associated with primary chemo-resistance and poor response to chemotherapy at diagnosis[60] and it is also abundantly expressed in SKOV-3 cells representing mesenchymal phenotype.[61] A recent finding in colorectal cancer[62] demonstrated that restored expression of OPCML led to inhibition of cell motility and invasiveness via negatively regulating EMT. This reversal of EMT phenotype might be mediated by dissociation of VIM from the rafts. VIM is frequently found in lipid rafts, being reported in 34 out of 67 raft proteomes in RaftProt[23] including prostate, breast cancer, renal cell carcinoma and melanoma rafts. However, further studies are required to determine the molecular function of intermediate filaments in lipid rafts, and its role in EMT transition. PRPH, also known as tetraspanin-22, is a member of the tetraspanin family that play a crucial role in cell adhesion.[63] Initially identified for its role in retinal photoreceptors and involvement in retinitis pigementosa,[64] PRPH has membrane fusion function.[65] According to the human protein atlas,[66] PRPH shows tissue selective expression, with low/medium protein expression in ovarian tumors but not expressed in normal ovary.

The extent of interconnectivity observed among the raft localized proteins of the ovarian cancer, prostate cancer and RCC lipid raft proteome supported the notion of lipid raft serving as a protein sorting platform. Biophysical evidence demonstrated a role for cholesterol and saturated sphingolipids in the enhancement of lipid raft rigidity.[67] This suggests that the raft compartmentalization of proteins might provide favorable environment to facilitate

interactions among raft components. Microdomains can act as a scaffold to concentrate molecules like receptors, adaptors, scaffolding proteins, effectors, kinases and cytoskeletal machinery to trigger complex signaling events in cancer. Intriguingly, the network simulation results revealed significantly increased connectivity for cancer raft proteome compared to the general human raft proteome. Transmembrane proteins anchored to this membrane-skeleton "fence" further influence clustering of lipid raft proteins through immobilization and increases tendency of protein-protein interaction at cancer rafts, as suggested by Kusumi *et al.*[68] Taken together, our results suggest stabilized membrane microdomains, facilitated by increased recruitment of cytoskeletal proteins and greater molecular interactions on the lipid raft, are an integral and reversible step in cancer development.

CONCLUSIONS

Through integrative analysis, we identified pan-cancer molecular signatures common in cancer cell lipid rafts. This 'core cancer lipid raft' proteome show a high representation of cytoskeleton associated proteins. Conversely, tumor suppressors PTRF in PC3 prostate cancers and OPCML in SKOV3 ovarian cancer cells act by significantly attenuating cytoskeletal components of the lipid raft proteome. Furthermore, we found that cancer raft proteome has an increased potential for protein-protein interaction compared to general human raft proteome. Taken together, these results suggest that cancer development is associated with cytoskeletal rearrangements to stabilize raft platforms and promote raft associated molecular interactions. The fact that two independent tumor suppressors (PTRF and OPCML) reduced these interactions suggests disruption of cytoskeleton-lipid raft assemblies as a potential anti-cancer strategy. We believe the integrated approach we presented here will pave the way to more refined representation of lipid raft dynamics in various malignancies.

SUPPORTING INFORMATION

- Supplemental Table S1: Human cytoskeletal associated proteins along with their GO annotations used for enrichment analysis
- Supplemental Table S2: Altered protein list from published cancer lipid raft proteome datasets used for the comparative analysis
- Supplemental Table S3: Raw peptide summary document of quantitative proteomics analysis of ovarian cancer lipid raft upon wild type and mutant OPCML over-expression
- Supplemental Table S4: Protein expression profiles in ovarian cancer lipid raft upon wild type and mutant OPCML over-expression along with a list of unique DRM proteins identified in the ovarian lipid raft.
- Supplemental Table S5: Topological properties of networks generated using random sampling.
- Supplemental Figure S1: Distribution of protein ratios before and after normalization.
- Supplemental Figure S2: Protein-protein interaction network of ovarian lipid raft associated proteins. The nodes represent individual protein (183) and the lines connecting the nodes are physical interaction among them.

FUNDING SOURCES

We gratefully acknowledge the support of the Australian Research Council [FT120100251] to Michelle M. Hill and [DP160100224] to Michelle M. Hill and Alexandre S. Cristino for this work. Anup D. Shah is a recipient of the International Postgraduate Research Scholarship. Melissa J. Davis is funded by a National Breast Cancer Foundation fellowship ECF-14-043.

ACKNOWLEDGMENTS

We thank Dorothy Loo of Translational Research Institute Proteomics facility for technical support.

ABBREVIATIONS:

EOC, epithelial ovarian cancer; OPCML, opioid binding protein and cell adhesion molecule; PTRF, polymerase I and transcript release factor; RTK, receptor tyrosin kinase; Ig, immunoglobin; WT, wild type; SILAC, stable isotope labeling by amino acids in cell culture; DRM, detergent resistant membrane; MS, mass spectrometry; LC, liquid chromatography; QPPC, quantitative proteomics *p-value* calculator; GO, gene ontology; RCC, renal cell carcinoma; ANK, adjacent normal kidney; NF2,type 2 neurofibromatosis; EMT, epithelial to mesenchymal transition

REFERENCES

1. Hanahan, D.; Weinberg, R. A., Hallmarks of cancer: the next generation. *Cell* **2011,** *144* (5), 646-674.

2. Gupta, G. P.; Massagué, J., Cancer metastasis: building a framework. *Cell* **2006,** *127* (4), 679-695.

3. Staubach, S.; Hanisch, F.-G., Lipid rafts: signaling and sorting platforms of cells and their roles in cancer. *Expert Rev. Proteomics* **2011,** *8* (2), 263-277.

4. Irwin, M. E.; Mueller, K. L.; Bohin, N.; Ge, Y.; Boerner, J. L., Lipid raft localization of EGFR alters the response of cancer cells to the EGFR tyrosine kinase inhibitor gefitinib. *J. Cell. Physiol.* **2011,** *226* (9), 2316-2328.

5. Chinni, S. R.; Yamamoto, H.; Dong, Z.; Sabbota, A.; Bonfil, R. D.; Cher, M. L., CXCL12/CXCR4 transactivates HER2 in lipid rafts of prostate cancer cells and promotes growth of metastatic deposits in bone. *Mol. Cancer Res.* **2008,** *6* (3), 446-457.

6. Casaletto, J. B.; McClatchey, A. I., Spatial regulation of receptor tyrosine kinases in development and cancer. *Nat. Rev. Cancer* **2012,** *12* (6), 387-400.

7. Freeman, M. R.; Cinar, B.; Lu, M. L., Membrane rafts as potential sites of nongenomic hormonal signaling in prostate cancer. *Trends Endocrinol. Metab.* **2005,** *16* (6), 273-279.

8. Babina, I. S.; Donatello, S.; Nabi, I. R.; Hopkins, A. M. Lipid rafts as master regulators of breast cancer cell function 2011. http://epubs.rcsi.ie/surgart.

9. Zhang, Q.; Furukawa, K.; Chen, H.-H.; Sakakibara, T.; Urano, T.; Furukawa, K., Metastatic potential of mouse Lewis lung cancer cells is regulated via ganglioside GM1 by modulating the matrix metalloprotease-9 localization in lipid rafts. *J. Biol. Chem.* **2006,** *281* (26), 18145-18155.

10. Delmas, D.; Rébé, C.; Lacour, S.; Filomenko, R.; Athias, A.; Gambert, P.; Cherkaoui-Malki, M.; Jannin, B.; Dubrez-Daloz, L.; Latruffe, N., Resveratrol-induced apoptosis is associated with Fas redistribution in the rafts and the formation of a death-inducing signaling complex in colon cancer cells. *J. Biol. Chem.* **2003,** *278* (42), 41482-41490.

11. Caruso, J. A.; Stemmer, P. M., Proteomic profiling of lipid rafts in a human breast cancer model of tumorigenic progression. *Clin. Exp. Metastasis* **2011,** *28* (6), 529-540.

12. Baruthio, F.; Quadroni, M.; Rüegg, C.; Mariotti, A., Proteomic analysis of membrane rafts of melanoma cells identifies protein patterns characteristic of the tumor progression stage. *Proteomics* **2008,** *8* (22), 4733-4747.

13. Raimondo, F.; Corbetta, S.; Savoia, A.; Chinello, C.; Cazzaniga, M.; Rocco, F.; Bosari, S.; Grasso, M.; Bovo, G.; Magni, F.; Pitto, M., Comparative membrane proteomics: a

technical advancement in the search of renal cell carcinoma biomarkers. *Mol. Biosyst.* **2015,** *11* (6), 1708-1716.

14. Inder, K. L.; Zheng, Y. Z.; Davis, M. J.; Moon, H.; Loo, D.; Nguyen, H.; Clements, J. A.; Parton, R. G.; Foster, L. J.; Hill, M. M., Expression of PTRF in PC-3 cells modulates cholesterol dynamics and the actin cytoskeleton impacting secretion pathways. *Mol. Cell. Proteomics* **2012,** *11* (2), M111. 012245.

15. Moon, H.; Lee, C.; Inder, K.; Sharma, S.; Choi, E.; Black, D.; Le Cao, K.; Winterford, C.; Coward, J.; Ling, M., PTRF/cavin-1 neutralizes non-caveolar caveolin-1 microdomains in prostate cancer. *Oncogene* **2014,** *33* (27), 3561-3570.

16. Stickney, J. T.; Bacon, W. C.; Rojas, M.; Ratner, N.; Ip, W., Activation of the tumor suppressor merlin modulates its interaction with lipid rafts. *Cancer Res.* **2004,** *64* (8), 2717-2724.

17. Ntougkos, E.; Rush, R.; Scott, D.; Frankenberg, T.; Gabra, H.; Smyth, J. F.; Sellar, G. C., The IgLON family in epithelial ovarian cancer: expression profiles and clinicopathologic correlates. *Clin. Cancer Res.* **2005,** *11* (16), 5764-5768.

18. Sellar, G. C.; Watt, K. P.; Rabiasz, G. J.; Stronach, E. A.; Li, L.; Miller, E. P.; Massie, C. E.; Miller, J.; Contreras-Moreira, B.; Scott, D., OPCML at 11q25 is epigenetically inactivated and has tumor-suppressor function in epithelial ovarian cancer. *Nat. Genet.* **2003,** *34* (3), 337-343.

19. Cancer Genome Atlas Research Network. Integrated genomic analyses of ovarian carcinoma. *Nature* **2011,** *474* (7353), 609-615.

20. McKie, A. B.; Vaughan, S.; Zanini, E.; Okon, I. S.; Louis, L.; de Sousa, C.; Greene, M. I.; Wang, Q.; Agarwal, R.; Shaposhnikov, D., The OPCML tumor suppressor Functions

as a cell surface repressor–adaptor, Negatively regulating receptor tyrosine Kinases in epithelial Ovarian cancer. *Cancer Discov.* **2012,** *2* (2), 156-171.

21. Zhou, F.; Tao, G.; Chen, X.; Xie, W.; Liu, M.; Cao, X., Methylation of OPCML promoter in ovarian cancer tissues predicts poor patient survival. *Clin. Chem. Lab. Med.* **2014,** *52* (5), 735-742.

22. Wu, S. Y.; Sood, A. K., New roles opined for OPCML. *Cancer Discov.* **2012,** *2* (2), 115-116.

23. Shah, A.; Chen, D.; Boda, A. R.; Foster, L. J.; Davis, M. J.; Hill, M. M., RaftProt: mammalian lipid raft proteome database. *Nucleic Acids Res.* **2015,** *43* (D1), D335-D338.

24. Carbon, S.; Ireland, A.; Mungall, C. J.; Shu, S.; Marshall, B.; Lewis, S., AmiGO: online access to ontology and annotation data. *Bioinformatics* **2009,** *25* (2), 288-289.

25. Moon, H.; Ruelcke, J. E.; Choi, E.; Sharpe, L. J.; Nassar, Z. D.; Bielefeldt-Ohmann, H.; Parat, M.-O.; Shah, A.; Francois, M.; Inder, K. L., Diet-induced hypercholesterolemia promotes androgen-independent prostate cancer metastasis via IQGAP1 and caveolin-1. *Oncotarget* **2015,** *6* (10), 7438.

26. Inder, K. L.; Loo, D.; Zheng, Y. Z.; Parton, R. G.; Foster, L. J.; Hill, M., Normalization of protein at different stages in SILAC subcellular proteomics affects functional analysis. *J. Integr. OMICS* **2012,** *2* (2), 114-122.

27. Zheng, Y. Z.; Boscher, C.; Inder, K. L.; Fairbank, M.; Loo, D.; Hill, M. M.; Nabi, I. R.; Foster, L. J., Differential impact of caveolae and caveolin-1 scaffolds on the membrane raft proteome. *Mol. Cell. Proteomics* **2011,** *10* (10), M110. 007146.

28. Foster, L. J.; de Hoog, C. L.; Mann, M., Unbiased quantitative proteomics of lipid rafts reveals high specificity for signaling factors. *Proceedings of the National Academy of Sciences* **2003,** *100* (10), 5813-5818.

29. Lingwood, D.; Simons, K., Detergent resistance as a tool in membrane research. *Nat. Protoc.* **2007,** *2* (9), 2159-2165.

30. Pike, L. J.; Han, X.; Chung, K.-N.; Gross, R. W., Lipid rafts are enriched in arachidonic acid and plasmenylethanolamine and their composition is independent of caveolin-1 expression: a quantitative electrospray ionization/mass spectrometric analysis. *Biochemistry* **2002,** *41* (6), 2075-2088.

31. The Common Repository of Adventitious Proteins (cRAP) Database. ftp://ftp.thegpm.org/fasta/cRAP (accessed Aug 18, 2014).

32. Chen, D.; Shah, A.; Nguyen, H.; Loo, D.; Inder, K. L.; Hill, M. M., Online quantitative proteomics p-value calculator for permutation-based statistical testing of peptide ratios. *J. Proteome Res.* **2014,** *13* (9), 4184-4191.

33. Nguyen, H. D.; Wood, I.; Hill, M. M., A robust permutation test for quantitative SILAC proteomics experiments. *J. Integr. OMICS* **2012,** *2* (2), 80-93.

34. Cowley, M. J.; Pinese, M.; Kassahn, K. S.; Waddell, N.; Pearson, J. V.; Grimmond, S. M.; Biankin, A. V.; Hautaniemi, S.; Wu, J., PINA v2. 0: mining interactome modules. *Nucleic Acids Res.* **2011**, gkr967.

35. Prasad, T. K.; Goel, R.; Kandasamy, K.; Keerthikumar, S.; Kumar, S.; Mathivanan, S.; Telikicherla, D.; Raju, R.; Shafreen, B.; Venugopal, A., Human protein reference database—2009 update. *Nucleic Acids Res.* **2009,** *37* (suppl 1), D767-D772.

36. Kerrien, S.; Aranda, B.; Breuza, L.; Bridge, A.; Broackes-Carter, F.; Chen, C.; Duesbury, M.; Dumousseau, M.; Feuermann, M.; Hinz, U., The IntAct molecular interaction database in 2012. *Nucleic Acids Res.* **2011**, gkr1088.

37. Chatr-aryamontri, A.; Breitkreutz, B.-J.; Oughtred, R.; Boucher, L.; Heinicke, S.; Chen, D.; Stark, C.; Breitkreutz, A.; Kolas, N.; O'Donnell, L., The BioGRID interaction database: 2015 update. *Nucleic Acids Res.* **2014**, gku1204.

38. Licata, L.; Briganti, L.; Peluso, D.; Perfetto, L.; Iannuccelli, M.; Galeota, E.; Sacco, F.; Palma, A.; Nardozza, A. P.; Santonico, E., MINT, the molecular interaction database: 2012 update. *Nucleic Acids Res.* **2012,** *40* (D1), D857-D861.

39. Salwinski, L.; Miller, C. S.; Smith, A. J.; Pettit, F. K.; Bowie, J. U.; Eisenberg, D., The database of interacting proteins: 2004 update. *Nucleic Acids Res.* **2004,** *32* (suppl 1), D449-D451.

40. Güldener, U.; Münsterkötter, M.; Oesterheld, M.; Pagel, P.; Ruepp, A.; Mewes, H.-W.; Stümpflen, V., MPact: the MIPS protein interaction resource on yeast. *Nucleic Acids Res.* **2006,** *34* (suppl 1), D436-D441.

41. Cline, M. S.; Smoot, M.; Cerami, E.; Kuchinsky, A.; Landys, N.; Workman, C.; Christmas, R.; Avila-Campilo, I.; Creech, M.; Gross, B., Integration of biological networks and gene expression data using Cytoscape. *Nat. Protoc.* **2007,** *2* (10), 2366-2382.

42. Csardi, G.; Nepusz, T., The igraph software package for complex network research. *InterJournal, Complex Systems* **2006,** *1695* (5), 1-9.

43. Zhou, Y.; Liang, H.; Rodkey, T.; Ariotti, N.; Parton, R. G.; Hancock, J. F., Signal integration by lipid-mediated spatial cross talk between Ras nanoclusters. *Mol. Cell. Biol.* **2014,** *34* (5), 862-876.

44. Mueller, V.; Ringemann, C.; Honigmann, A.; Schwarzmann, G.; Medda, R.; Leutenegger, M.; Polyakova, S.; Belov, V.; Hell, S.; Eggeling, C., STED nanoscopy

reveals molecular details of cholesterol-and cytoskeleton-modulated lipid interactions in living cells. *Biophys. J.* **2011,** *101* (7), 1651-1660.

45. Gómez-Llobregat, J.; Buceta, J.; Reigada, R., Interplay of cytoskeletal activity and lipid phase stability in dynamic protein recruitment and clustering. *Sci. Rep.* **2013,** *3*, 2608.

46. Wickström, S. A.; Alitalo, K.; Keski-Oja, J., Endostatin associates with lipid rafts and induces reorganization of the actin cytoskeleton via down-regulation of RhoA activity. *J. Biol. Chem.* **2003,** *278* (39), 37895-37901.

47. Head, B. P.; Patel, H. H.; Insel, P. A., Interaction of membrane/lipid rafts with the cytoskeleton: impact on signaling and function: membrane/lipid rafts, mediators of cytoskeletal arrangement and cell signaling. *BBA-Biomembranes* **2014,** *1838* (2), 532-545.

48. Li, Y.; Kang, Y. S.; Dai, C.; Kiss, L. P.; Wen, X.; Liu, Y., Epithelial-to-mesenchymal transition is a potential pathway leading to podocyte dysfunction and proteinuria. *The American journal of pathology* **2008,** *172* (2), 299-308.

49. Kalluri, R.; Weinberg, R. A., The basics of epithelial-mesenchymal transition. *The Journal of clinical investigation* **2009,** *119* (6), 1420-1428.

50. Schlegel, N.; Meir, M.; Heupel, W.-M.; Holthöfer, B.; Leube, R. E.; Waschke, J., Desmoglein 2-mediated adhesion is required for intestinal epithelial barrier integrity. *Am. J. Physiol. Gastrointest. Liver Physiol.* **2010,** *298* (5), G774-G783.

51. Nicolau, D. V.; Burrage, K.; Parton, R. G.; Hancock, J. F., Identifying optimal lipid raft characteristics required to promote nanoscale protein-protein interactions on the plasma membrane. *Mol. Cell. Biol.* **2006,** *26* (1), 313-323.

52. Byrum, J. N.; Rodgers, W., Membrane-cytoskeleton interactions in cholesterol-dependent domain formation. *Essays Biochem.* **2015,** *57*, 177-187.

53. Türkcan, S.; Richly, M. U.; Alexandrou, A.; Masson, J.-B., Probing membrane protein interactions with their lipid raft environment using single-molecule tracking and Bayesian inference analysis. *PLoS One* **2013,** *8* (1), e53073.

54. Fife, C.; McCarroll, J.; Kavallaris, M., Movers and shakers: cell cytoskeleton in cancer metastasis. *Br. J. Pharmacol.* **2014,** *171* (24), 5507-5523.

55. Chichili, G. R.; Rodgers, W., Cytoskeleton–membrane interactions in membrane raft structure. *Cell. Mol. Life Sci.* **2009,** *66* (14), 2319-2328.

56. Nicolson, G. L., Cell Membrane Fluid–Mosaic Structure and Cancer Metastasis. *Cancer Res.* **2015,** *75* (7), 1169-1176.

57. Viola, A.; Gupta, N., Tether and trap: regulation of membrane-raft dynamics by actin-binding proteins. *Nat. Rev. Immunol.* **2007,** *7* (11), 889-896.

58. McClatchey, A. I.; Giovannini, M., Membrane organization and tumorigenesis—the NF2 tumor suppressor, Merlin. *Genes Dev.* **2005,** *19* (19), 2265-2277.

59. Vuoriluoto, K.; Haugen, H.; Kiviluoto, S.; Mpindi, J.; Nevo, J.; Gjerdrum, C.; Tiron, C.; Lorens, J.; Ivaska, J., Vimentin regulates EMT induction by Slug and oncogenic H-Ras and migration by governing Axl expression in breast cancer. *Oncogene* **2011,** *30* (12), 1436-1448.

60. Davidson, B.; Holth, A.; Hellesylt, E.; Tan, T. Z.; Huang, R. Y.-J.; Tropé, C.; Nesland, J. M.; Thiery, J. P., The clinical role of epithelial-mesenchymal transition and stem cell markers in advanced-stage ovarian serous carcinoma effusions. *Hum. Pathol.* **2015,** *46* (1), 1-8.

61. Yi, B.-R.; Kim, T.-H.; Kim, Y.-S.; Choi, K.-C., Alteration of epithelial-mesenchymal transition markers in human normal ovaries and neoplastic ovarian cancers. *Int. J. Oncol.* **2015,** *46* (1), 272-280.

62. Li, C.; Tang, L.; Zhao, L.; Li, L.; Xiao, Q.; Luo, X.; Peng, W.; Ren, G.; Tao, Q.; Xiang, T., OPCML is frequently methylated in human colorectal cancer and its restored expression reverses EMT via downregulation of smad signaling. *Am. J. Cancer Res.* **2015,** *5* (5), 1635.

63. Lazo, P. A., Functional implications of tetraspanin proteins in cancer biology. *Cancer Sci.* **2007,** *98* (11), 1666-1677.

64. Ritter, L. M.; Boesze-Battaglia, K.; Tam, B. M.; Moritz, O. L.; Khattree, N.; Chen, S.-C.; Goldberg, A. F., Uncoupling of Photoreceptor Peripherin/rds Fusogenic Activity from Biosynthesis, Subunit Assembly, and Targeting a Potential Mechnism for Pathogenic Effects. *J. Biol. Chem.* **2004,** *279* (38), 39958-39967.

65. Lee, E. S.; Burnside, B.; Flannery, J. G., Characterization of peripherin/rds and rom-1 transport in rod photoreceptors of transgenic and knockout animals. *Invest. Ophthalmol. Vis. Sci.* **2006,** *47* (5), 2150.

66. Uhlén, M.; Fagerberg, L.; Hallström, B. M.; Lindskog, C.; Oksvold, P.; Mardinoglu, A.; Sivertsson, Å.; Kampf, C.; Sjöstedt, E.; Asplund, A., Tissue-based map of the human proteome. *Science* **2015,** *347* (6220), 1260419.

67. Orädd, G.; Shahedi, V.; Lindblom, G., Effect of sterol structure on the bending rigidity of lipid membranes: A 2 H NMR transverse relaxation study. *BBA-Biomembranes* **2009,** *1788* (9), 1762-1771.

68. Kusumi, A.; Nakada, C.; Ritchie, K.; Murase, K.; Suzuki, K.; Murakoshi, H.; Kasai, R. S.; Kondo, J.; Fujiwara, T., Paradigm shift of the plasma membrane concept from the two-dimensional continuum fluid to the partitioned fluid: high-speed single-molecule tracking of membrane molecules. *Annu. Rev. Biophys. Biomol. Struct.* **2005,** *34*, 351-378.

FIGURE LEGENDS

Figure1: Schematic representation of integrative analysis of lipid raft proteomes in multiple cancer progression and tumor suppression models to identify pan-cancer lipid raft proteomic signatures.

Figure 2: Overlap between differentially expressed lipid raft residing proteins during cancer progression. (a) Up-regulated proteins in aggressive cancer phenotypes (b) Down-regulated proteins in aggressive cancer phenotypes identified in breast cancer, renal cell carcinoma and melanoma lipid raft proteomics datasets.

Figure 3: OPCML regulates lipid raft proteome. (a) Triplex SILAC quantitative subcellular lipid raft proteomics experiment workflow. (b) Domain architecture of OPCML showing three immunoglobulin-like domains along with the location of somatic missense P95R mutation on the first immunoglobin (Ig) like domain. (c) 3D homology model of the first Ig domain of OPCML with replacement of Proline to Arginine residue at the surface of loop between two beta sheets. (d) Volcano plot showing magnitude and significance of the lipid raft protein level changes in control SKOV3 cells compared to WT OPCML expressing SKOV3 cells. The vertical axis indicates –log(*p-value*). The horizontal axis indicates log(fold change). Proteins satisfy the fold change criteria represented by orange and proteins passed the *p-value* cut-off were shown in blue color. The differentially expressed proteins meeting both criteria are shown in magenta color. (e) Volcano plot showing magnitude and significance of the lipid raft protein levels in control SKOV3 cells compared to P95R OPCML expressing SKOV3 cells. (f) Overlap between WT OPCML and P95R OPCML regulated lipid raft proteins in SKOV3 cells.

Figure 4: Expression signatures of cytoskeleton associated proteins at ovarian lipid rafts upon WT and P95R OPCML expression in SKOV3 cells. Pair-wise comparison between (a) Control SKOV3 (OPCML negative) versus WT OPCML (b) Control SKOV3 (OPCML negative)

versus P95R OPCML. A sub-network of WT OPCML regulated cytoskeleton associated proteins is shown in (c), and the effect of P95R OPCML expression on these proteins shown in (d). Magenta colored proteins are down-regulated with fold change ≤-1.5; up-regulated protein with fold change threshold of ≥ 1.5 represented by green; gray colored proteins for which ratio was not found. Thicker borders indicate significantly altered proteins (p-value < 0.05).

Figure 5: OPCML mediated altered expression of binding partners of significantly different cytoskeletal proteins. Interactions between binding partners of significantly altered cytoskeletal proteins (VIM, PRPH, DES, PLEC, JUP and SPTAN1) by WT OPCML. Comparison between (a) Control SKOV3 (OPCML negative) versus WT OPCML (b) Control SKOV3 (OPCML negative) versus P95R OPCML. Magenta colored proteins are down-regulated proteins with fold change ≤ -1.5; up-regulated protein with fold change threshold of ≥1.5 represented by green; gray colored proteins found to dissociate from ovarian lipid rafts in the respective comparison and the proteins with thicker borders are significantly altered proteins (permutation p-value<0.05) in each pair-wise comparison. Cytoskeleton associated proteins are represented by diamond shape.

FIGURES

Figure 1

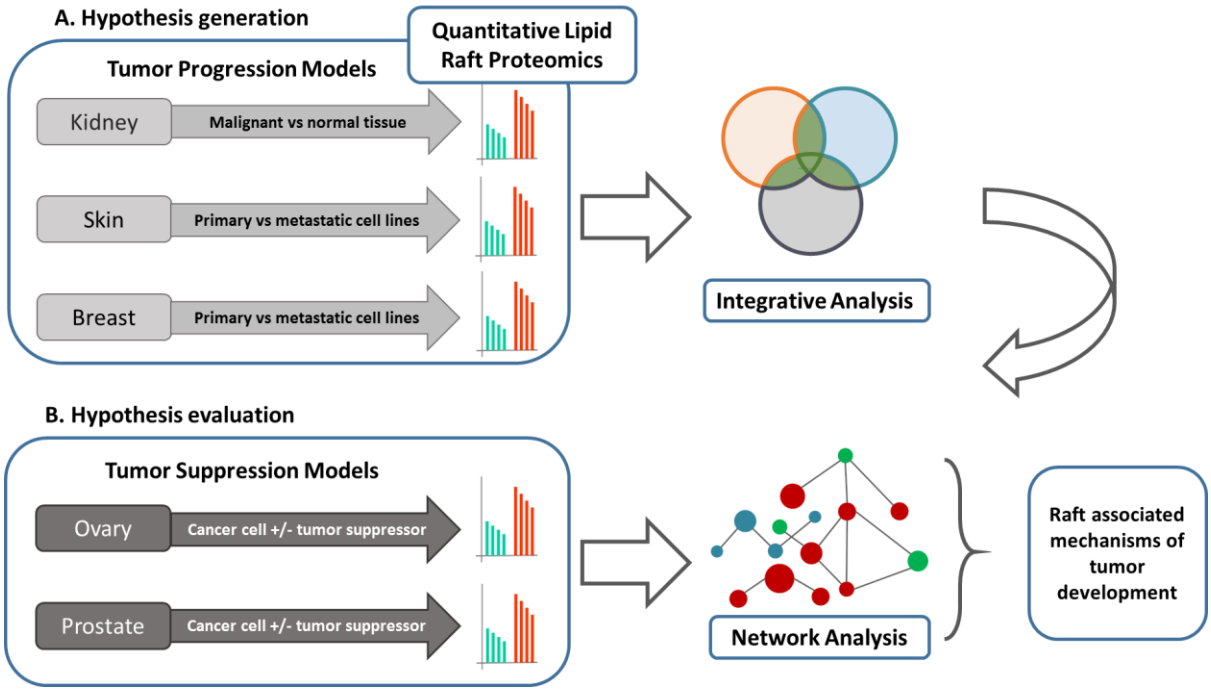

Figure 2

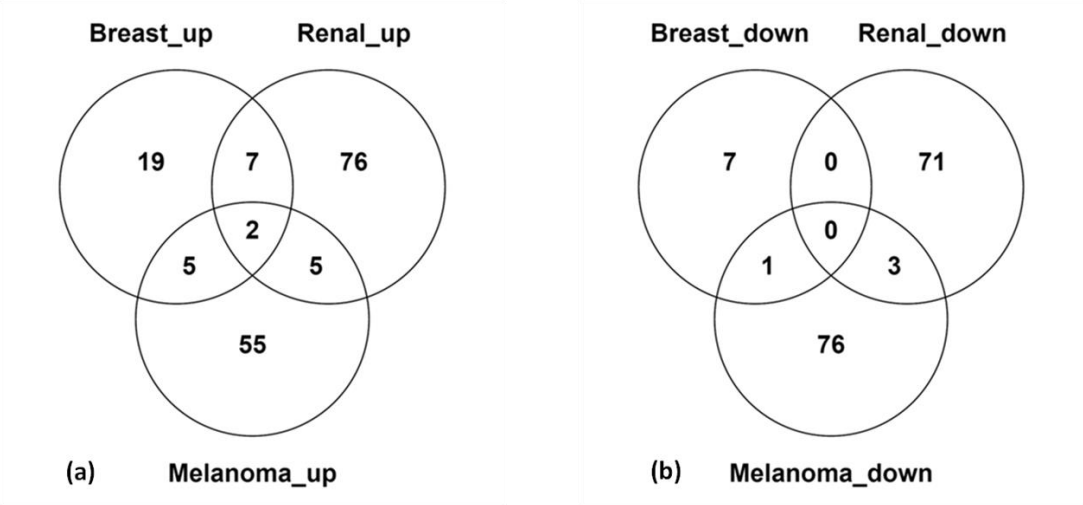
Breast_up
Renal_up
19
7
76
2
5
5
55
(a)
Melanoma_up
Breast_down
Renal_down
7
0
71
0
1
3
76
(b)
Melanoma_down

Figure 3

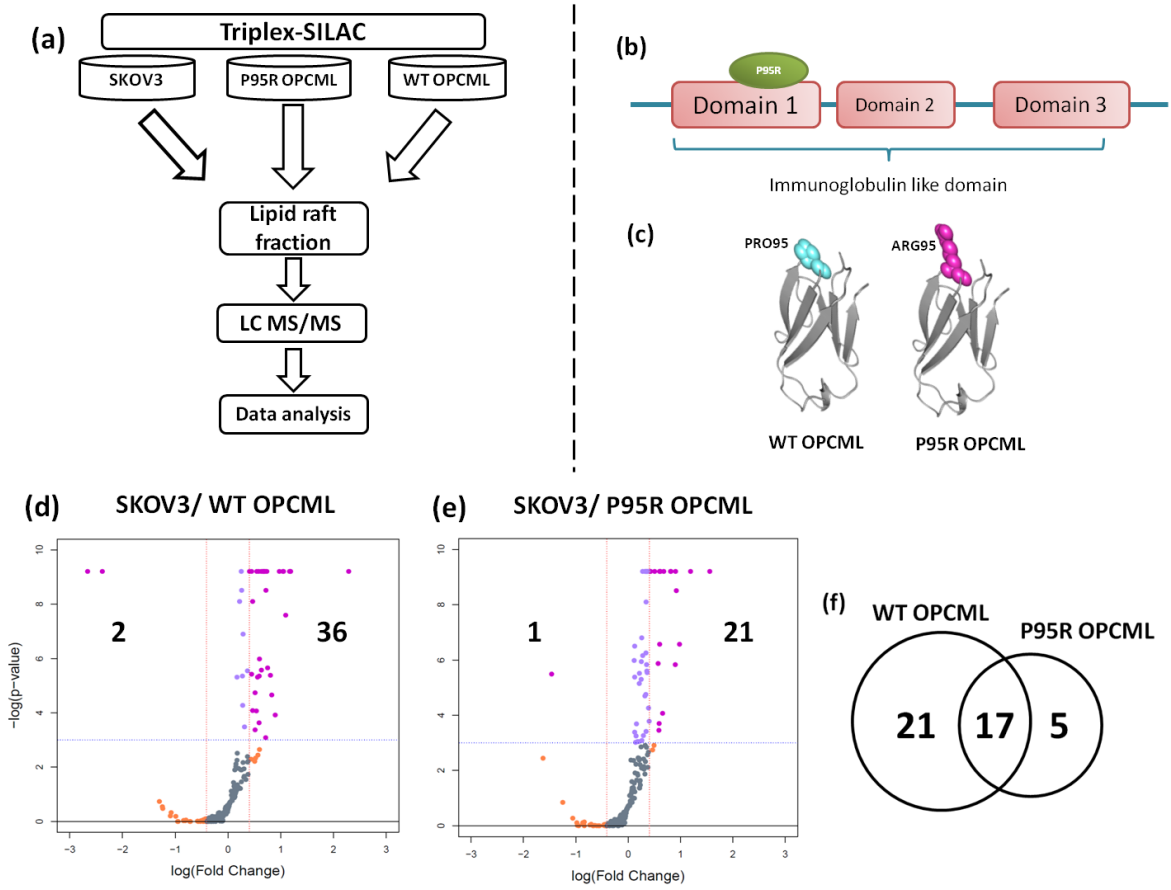
(a)
Triplex-SILAC
SKOV3
P95R OPCML
WT OPCML
Lipid raft fraction
LC MS/MS
Data analysis
(b)
P95R
Domain 1
Domain 2
Domain 3
Immunoglobulin like domain
(c)
PRO95
ARG95
WT OPCML
P95R OPCML
(d)
SKOV3/ WT OPCML
2
36
−log(p-value)
log(Fold Change)
(e)
SKOV3/ P95R OPCML
1
21
log(Fold Change)
(f)
WT OPCML
P95R OPCML
21
17
5

Figure 4

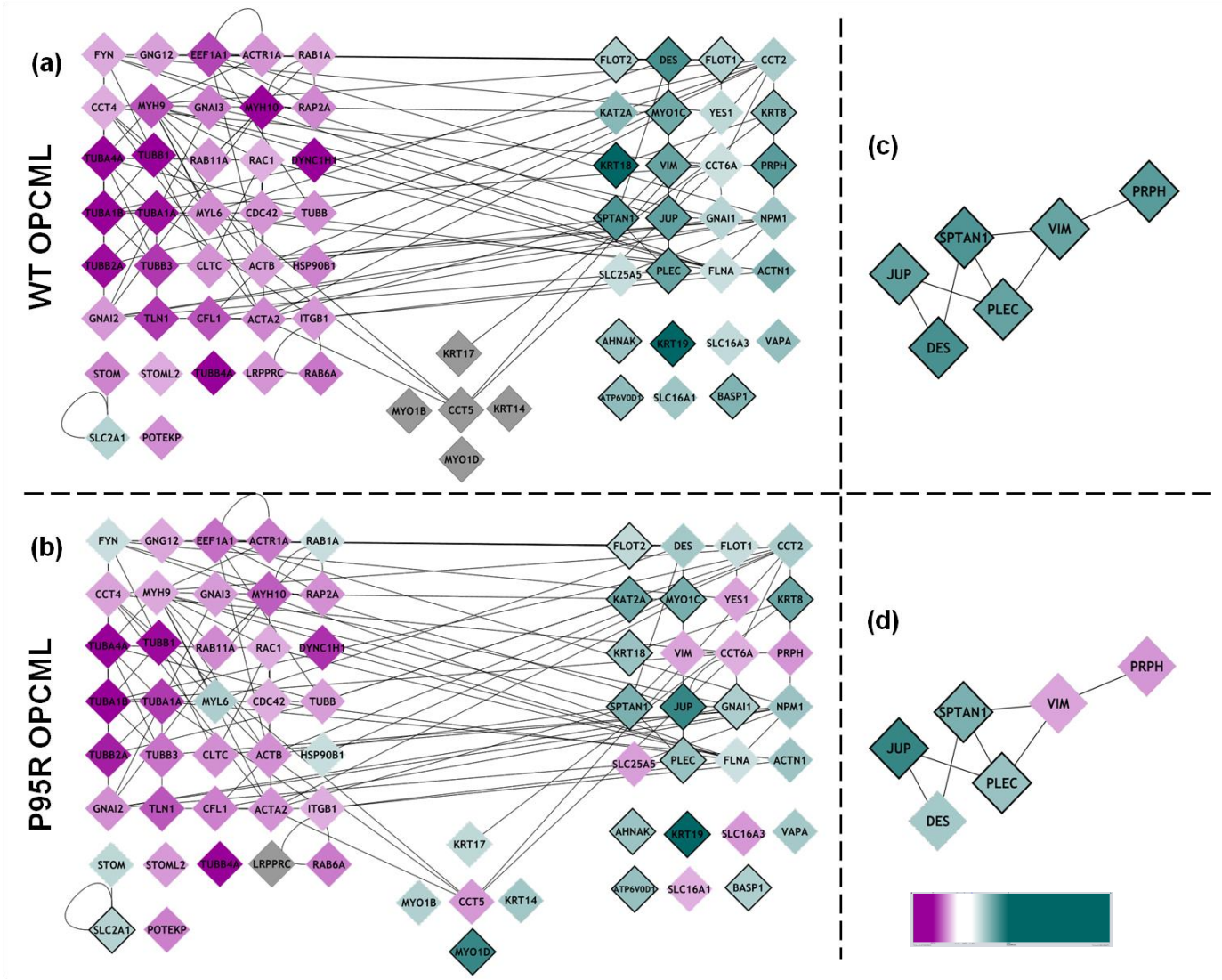
(a)
WT OPCML
FYN
GNG12
EEF1A1
ACTR1A
RAB1A
CCT4
MYH9
GNAI3
MYH10
RAP2A
TUBA4A
TUBB1
RAB11A
RAC1
DYNC1H1
TUBA1B
TUBA1A
MYL6
CDC42
TUBB
TUBB2A
TUBB3
CLTC
ACTB
HSP90B1
GNAI2
TLN1
CFL1
ACTA2
ITGB1
STOM
STOML2
TUBB4A
LRPPRC
RAB6A
SLC2A1
POTEKP
KRT17
MYO1B
CCT5
KRT14
MYO1D
FLOT2
DES
FLOT1
CCT2
KAT2A
MYO1C
YES1
KRT8
KRT18
VIM
CCT6A
PRPH
SPTAN1
JUP
GNAI1
NPM1
SLC25A5
PLEC
FLNA
ACTN1
AHNAK
KRT19
SLC16A3
VAPA
ATP6V0D1
SLC16A1
BASP1
(b)
P95R OPCML
(c)
PRPH
SPTAN1
VIM
JUP
PLEC
DES
(d)
PRPH
SPTAN1
VIM
JUP
PLEC
DES

Figure 5

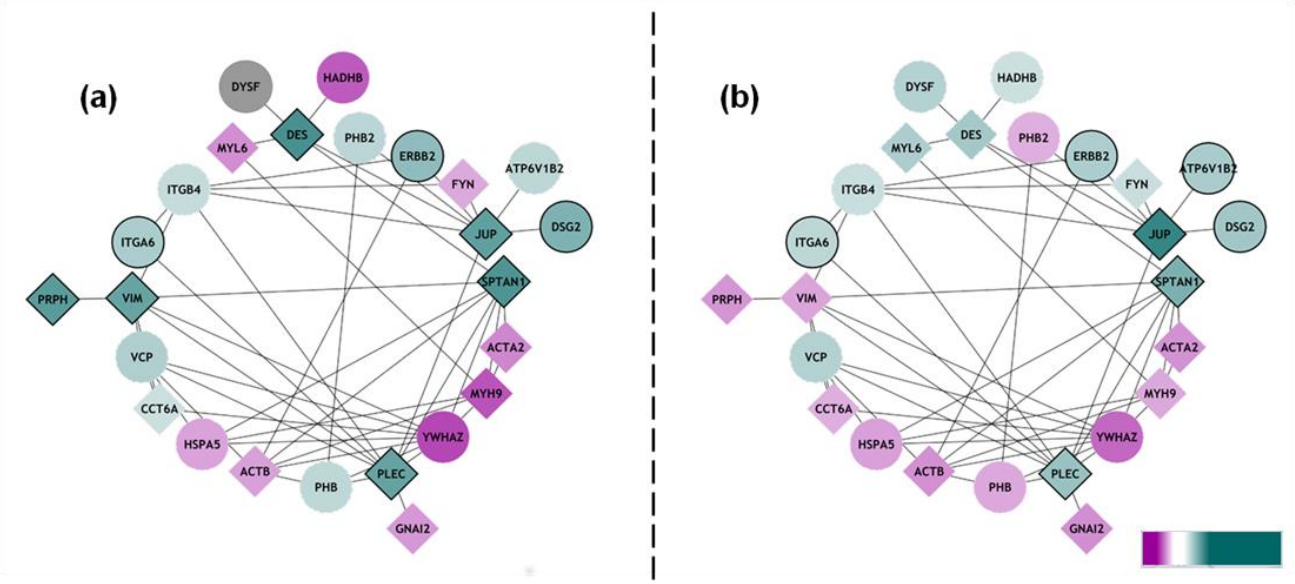
(a)
DYSF
HADHB
DES
MYL6
PHB2
ERBB2
ATP6V1B2
FYN
ITGB4
DSG2
JUP
ITGA6
SPTAN1
PRPH
VIM
ACTA2
VCP
MYH9
CCT6A
YWHAZ
HSPA5
ACTB
PLEC
PHB
GNAI2
(b)
DYSF
HADHB
DES
MYL6
PHB2
ERBB2
ATP6V1B2
FYN
ITGB4
DSG2
JUP
ITGA6
SPTAN1
PRPH
VIM
ACTA2
VCP
MYH9
CCT6A
YWHAZ
HSPA5
ACTB
PLEC
PHB
GNAI2

TABLES:

Table 1: Proteins with increased and decreased expression at lipid raft in more aggressive cancer cells primary cells in two out of three cancer datasets

Protein Accession	Gene symbol	Protein name	Breast Cancer [11]	Melanoma [12]	Renal Cell Carcinoma [13]	Ovarian Cancer
Proteins enriched in more aggressive tumour derived rafts						
P68363	*TBA1B*	*Tubulin alpha-1B chain*	*Yes*	*No*	*Yes*	*Yes*
P04899	*GNAI2*	*Guanine nucleotide-binding protein G(i) subunit alpha-2*	*Yes*	*No*	*Yes*	*Yes*
P07355	ANXA2	Annexin A2 (Annexin II)	Yes	No	Yes	Yes
P08754	*GNAI3*	*Guanine nucleotide-binding protein G(k) subunit alpha*	*Yes*	*No*	*Yes*	*Yes*
P13987	CD59	CD59 glycoprotein (1F5 antigen)	Yes	No	Yes	Yes
Q03135	CAV1	Caveolin-1	Yes	No	Yes	Yes
Q9UBI6	*GBG12*	*Guanine nucleotide-binding protein G(I)/G(S)/G(O) subunit gamma-12*	*Yes*	*No*	*Yes*	*No*
P11142	HSP7C	Heat shock cognate 71 kDa protein	Yes	Yes	Yes	Yes
P35232	PHB	Prohibitin	Yes	Yes	Yes	Yes
P27105	*STOM*	*Erythrocyte band 7 integral membrane protein*	*No*	*Yes*	*Yes*	*Yes*
Q14254	*FLOT2*	*Flotillin-2*	*No*	*Yes*	*Yes*	*Yes*
P04406	*GAPDH*	*Glyceraldehyde-3-phosphate dehydrogenase*	*No*	*Yes*	*Yes*	*No*
P63000	*RAC1*	*Ras-related C3 botulinum toxin substrate 1*	*No*	*Yes*	*Yes*	*Yes*
P06396	*GELS*	*Gelsolin*	*No*	*Yes*	*Yes*	*No*

P62424	RL7A	60S ribosomal protein L7a	Yes	Yes	No	No
Q09666	*AHNAK*	*Neuroblast differentiation-associated protein AHNAK (Desmoyokin)*	*Yes*	*Yes*	*No*	*Yes*
Q13488	VPP3	V-type proton ATPase 116 kDa subunit a isoform 3	Yes	Yes	No	Yes
Q14126	DSG2	Desmoglein-2	Yes	Yes	No	Yes
Q99623	PHB2	Prohibitin-2	Yes	Yes	No	Yes
Proteins depleted from more aggressive tumour derived rafts						
Q15149	*PLEC*	*Plectin*	*Yes*	*Yes*	*No*	*Yes*
P15144	AMPN	Aminopeptidase N (plasma membrane glycoprotein CD13)	No	Yes	Yes	No
Q9NQ84	GPC5C	G-protein coupled receptor family C group 5 member C	No	Yes	Yes	Yes
P14625	*ENPL*	*Endoplasmin (Tumor rejection antigen 1)*	*No*	*Yes*	*Yes*	*Yes*

Proteins in *italics* are reported to be structural, regulatory or effector components of cytoskeleton.

Table 2: Enrichment of cytoskeletal associated protein in the ovarian lipid raft proteome and ovarian lipid raft associated interactome

Dataset	Background	# Cytoskeletal proteins	Total # proteins	X-squared	*p-value**
Ovarian lipid-raft proteome	Human lipid raft associated proteins	79	230	11.44	0.0007
Ovarian lipid raft associated protein-protein interactions	Human lipid raft associated proteins	69	183	11.78	0.0006
Ovarian lipid-raft proteome	Human proteome	79	230	26.87	2.17×10^{-07}
Ovarian lipid raft associated protein-protein interactions	Human proteome	69	183	25.06	5.55×10^{-07}

*Pearson's X^2 goodness of fit test against different background sets

Table 3: Topological properties of various protein-protein interaction networks

Topological Property	Human lipid raft proteins* (Total=4243)	Human proteome* (Total=20192)	Ovarian cancer lipid raft proteome (Total = 230)	Prostate cancer lipid raft proteome* (Total=358)	Renal cell carcinoma raft proteome* (Total=330)
Number of Proteins	80	34 p-value= 9.54×10^{-8}	183 p-value=3.35×10^{-68}	173 p-value= 5.29×10^{-58}	163 p-value= 1.72×10^{-51}
Number of Interactions	97	30 p-value= 1.4×10^{-12}	509 p-value= 0.00	460 p-value= 4.67×10^{-14}	378 p-value= 4.68×10^{-16}
Average Degree	2.40	1.71 p-value= 0.31	5.56 p-value= 7.80×10^{-97}	5.32 p-value= 1.93×10^{-12}	4.46 p-value= 1.21×10^{-10}

*The value of each topological property is an average value of 1000 networks generated by random sampling where the size of each dataset was normalized to number of proteins identified in the ovarian cancer lipid raft proteome.

The *p-value* is based on one tailed Z-test that compared average topological property of human raft protein-protein networks with the protein-protein interaction networks of each respective datasets.